ABSTRACT

2 Background

- 3 How experience and individuality shape action selection remains a major question in
- 4 neuroscience. Visually-evoked escape behavior within *Drosophila melanogaster* provides a
- 5 robust model to study these mechanisms within neural circuits but requires novel assays to
- 6 circumvent limitations of current behavior assays.

78 *Method*

- 9 Here we describe and characterize a simple, low to moderate cost, and flexible assay for
- studying visually-evoked escape responses in tethered flies. This assay consists of a DLP
- projector, cylindrical rear projection screen, and an automated flight interruption motor all
- controlled within a MATLAB environment.

13 14

1

Results

- We find this assay effectively recapitulates fly behaviors previously observed in free behavior
- assays, and provides a novel opportunity to investigate the behavior of individual flies over the
- 17 course of numerous stimulus presentations.

18 19

Comparison to existing methods

- 20 Current *Drosophila* escape assays do not permit multiple stimulus presentations and can be
- 21 highly complex and expensive to implement.

22 23

Conclusions

- 24 This assay provides an effective system to further identify neural components and mechanisms
- 25 underlying action selection within parallel sensorimotor pathways.

26

- 27 Keywords: action selection, behavioral assay, escape behavior, *Drosophila melanogaster*,
- 28 sensorimotor, neural circuits

29

30 Abbreviations: wingbeat tachometer (WBT), giant fibers (GF)

INTRODUCTION

A major focus in neuroscience research seeks to understand circuit mechanisms responsible for executing action selection. While certain action selection tasks may involve complex circuit interactions associated with higher cognition, others are performed in relatively simple sensorimotor pathways. By studying these sensorimotor circuits at single-cell resolution, we gain insight into how this class of action selection circuits function and illuminate principles of decision making circuits in general.

Escape and predator avoidance are particularly fruitful for evaluating the neural mechanisms behind action selection. Escape responses are robust and easily elicited in a laboratory setting (Card and Dickinson, 2008; Eaton et al., 1977; Hemmi and Tomsic, 2015; Holmqvist and Srinivasan, 1991; Yilmaz, 2013). Neural circuits underlying escape behavior are partially identified and amenable to calcium imaging or electrophysiological investigation (Eaton et al., 1991; Gabbiani et al., 1999; Herberholz, 2009; Klapoetke et al., 2017; Liu and Fetcho, 1999; Oliva and Torralba, 2007). Additionally, action selection during predation is more complex than a choice of whether or not to escape and instead consists of selecting among multiple escape response patterns (De Franceschi et al., 2016; Edwards et al., 1999; von Reyn et al., 2014) that can be modulated by specific properties of a predator stimulus, e.g. stimulus approach direction (Card and Dickinson, 2008; Dunn et al., 2016; Hemmi and Pfeil, 2010).

For example, the fruit fly *Drosophila melanogaster* utilizes parallel sensorimotor circuits to select between at least two kinematically distinct escape actions modulated by the apparent visual features of a predator's approach: a long preparation, stable escape takeoff or an unstable, short preparation takeoff (von Reyn et al., 2014). Across a population of flies, this distribution of short and long takeoffs becomes biased towards short preparation escapes as approach parameters are more abrupt (von Reyn et al., 2014). A wealth of behavioral data along with the breadth and specificity of available genetic reagents in *Drosophila* (Brand and Perrimon, 1993; Lai and Lee, 2006; Pfeiffer et al., 2008, 2010) have enabled circuit components of the escape response to be identified and manipulated with the utmost specificity (Allen et al., 2006; de Vries and Clandinin, 2012; Klapoetke et al., 2017; von Reyn et al., 2014, 2017). To date, however, action selection has only been investigated in free behavior assays limited to a single escape event (Card and Dickinson, 2008; de Vries and Clandinin, 2012; Fotowat et al., 2009; von Reyn et al., 2014; Trimarchi and Schneiderman, 1995). How the bimodal distribution changes across multiple stimulus presentations and is represented in the response of an individual fly remains unknown.

 Here, we take advantage that the fly's naturalistic escape response can be consistently and reliably induced in a laboratory setting to develop a tethered behavior assay that recapitulates the bimodal distribution of escapes witnessed in freely behaving flies. The presently developed system is unique in its combination of cost, simplicity, and flexibility in the repeated presentation of visual stimuli to tethered flies. As a tethered assay, it enables superior control of the stimulus presentation position relative to the fly's visual field. Additionally, by recording multiple responses from each fly, we gain the ability to directly investigate behavioral variability within individual flies as compared to the overall population.

In our assay, escapes are evoked visually by a looming stimulus, the two-dimensional 76 77 projection of an object approaching on a direct collision course with the fly. A variety of visual stimulus presentation assays have been developed for use in the study of visually mediated fly 78 79 behavior, both in tethered and freely behaving contexts. Display selection involves tradeoffs among resolution, refresh rate, luminance, contrast, flexibility of stimulus generation, and 80 implementation costs. Various technical solutions have been utilized in prior assays, including 81 LED, LCD, projection, modular designs, and coherent fiber optics, each with their various 82 advantages (Bahl et al., 2013; Card and Dickinson, 2008; Clark et al., 2011; Fotowat et al., 83 2009; Maimon et al., 2010; Reiser and Dickinson, 2008; Takalo et al., 2012). Here, in our 84 tethered assay, the use of standard projection equipment means that the simple, flexible, and 85 rapid generation of stimuli can be implemented through the use of any number of standard 3D 86 graphics packages while the use of a cylindrical projection surface provides a good balance 87 between simplicity of construction and visual field coverage. 88 89

Using this assay, we find that over the course of repeated stimulus presentation, flies show a rapid reduction in their escape response rate. Additionally, the probability of selecting each type of escape becomes biased towards long duration escapes as short duration responses attenuate more rapidly than long duration responses. Interestingly, we observe that rather than demonstrating a highly rigid response selection criterion across flies, individuals show significant variability in their response preferences. These data provide a basis for further investigations of circuit and genetic mechanisms underlying action selection in *Drosophila* escape. Furthermore, our assay increases the number of behavioral measures for escape, providing a useful tool for identifying novel neural components that may display mild phenotypes when genetically silenced or activated. Broadly, this assay provides an effective system to identify mechanisms underlying action selection within parallel sensorimotor pathways.

1. MATERIALS AND METHODS

2.1 Tethered escape assay

2.1.1 Assay components and configuration

The tethered escape assay consisted of a rear projection screen (double matte Mylar film) 107 attached to a cylindrical PVC frame (radius 2.25" and height 5") with a tethered fly positioned 108 at its focus (Figure 1A). Behavioral responses were recorded at 1300 fps by an IR camera (Point 109 Gray MP NIR Grasshopper 3 USB3.0 Camera, 1") and a wingbeat tachometer (WBT, 110 https://github.com/janelia-kicad/light sensor boards). For both the WBT and camera, 111 illumination was provided by 850nm LEDs that fall outside of the detection range for 112 Drosophila photoreceptors (Yamaguchi et al., 2010). To synchronize data acquisition, the 113 initial frame of the visual stimulus presentation was captured with a light sensitive diode and 114

calibrated to the WBT and IR camera. Between each trial, a motorized wingstop apparatus transiently interposed a flexible tube into the wing flight path to halt active flight. The entire

assay was surrounded in blackout material to avoid incidental lighting. Temperature and

humidity levels were actively monitored during the course of each experiment (Honeywell

119 HIH8121-021-001).

115

116

90

91 92

93

94 95

96

97

98

99

100

101 102 103

104

105

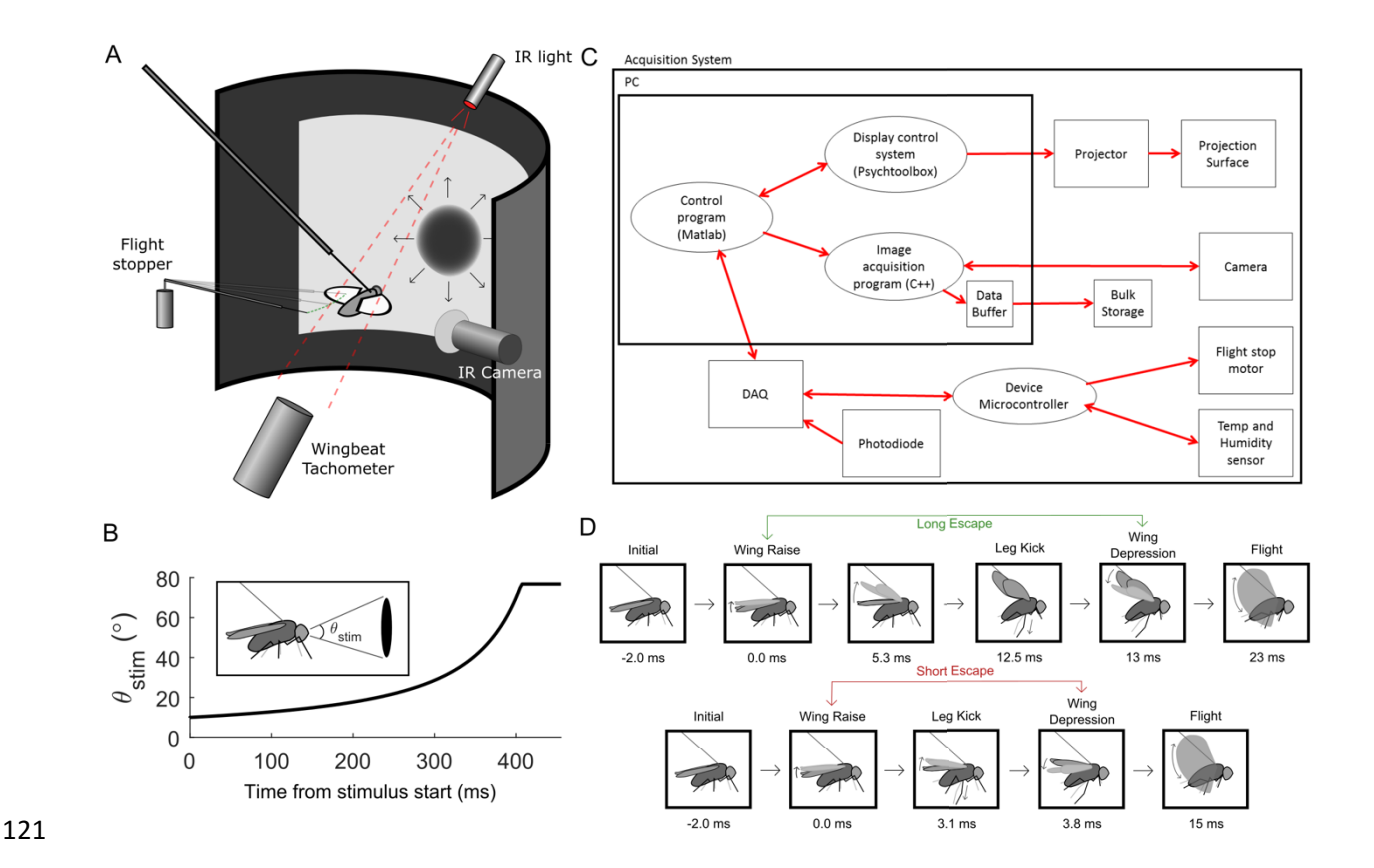


Figure 1: Visually-evoked tethered escape behavior assay. (A) Non-flying tethered flies are presented a looming stimulus, modeled after an object approaching at a constant velocity. A high speed IR camera records behavioral responses, a wingbeat tachometer records flight response characteristics, and a flight stop arm interrupts wing flight path following each trial. (B) Time course of stimulus expansion for r/v = 40 ms, from a 10° to 78° visual angle θ , with t = 0 at stimulus onset. (C) Data acquisition pathway for tethered assay. Data acquisition device was controlled using the Wavesurfer data acquisition package for MATLAB. Stimulus presentation timing was controlled using Psychtoolbox for MATLAB. (D) Annotated components of the escape sequence for both long or short duration escapes.

2.1.2 Display Parameters

Individual stimuli frames were projected onto the screen using a DLP projector (Texas Instruments DLP Lightcrafter 4500) at 400 Hz, a refresh rate substantively greater than the flicker fusion frequency of *Drosophila* (100Hz, Niven et al., 2003). To generate this refresh rate, the projector was configured to operate in pattern sequence mode where the 24bits of each 3 byte RGB image were divided into 4 greyscale image planes of 6 bits each across an 100Hz refresh rate.

Projected pixels were mapped to the projection surface by identifying the set of pixels p who's projected centers were incident on each of a grid of surface points in Cartesian space s and then finding the camera matrix R*K which minimizes the weighted squared error between p_i and the associated projection of a given surface point $f_{proj}(s_i)$. The matrix R consists of a rotation matrix

appended to the offset vector \vec{c} for the distance from the origin to the projector, with subscripts x, y, z representing the magnitude of the vector along each Cartesian coordinate.

136
$$Min\left(\sum_{i}^{n} w_{i} * \|p_{i} - f_{proj}([s_{i} \quad 1] * R * K)\|^{2}\right)$$
 (1.1)

137
$$f_{proj}(\vec{v}) = \begin{bmatrix} v_x & v_y \end{bmatrix} / v_z \tag{1.2}$$

138

139
$$R = \begin{bmatrix} \cos \beta \cos \gamma & \sin \alpha \sin \beta \cos \gamma - \cos \alpha \sin \gamma & \sin \alpha \sin \gamma + \cos \alpha \sin \beta \cos \gamma \\ \cos \beta \sin \gamma & \cos \alpha \cos \gamma + \sin \alpha \sin \beta \sin \gamma & \cos \alpha \sin \beta \sin \gamma - \cos \gamma \sin \alpha \\ -\sin \beta & \sin \alpha \cos \beta & \cos \alpha \cos \beta \\ \hline c_x & c_y & c_z \end{bmatrix}$$
(1.3)

140

141
$$K = \begin{bmatrix} f * ratio * d & 0 & 0 \\ 0 & f * d & 0 \\ px_x/2 & px_y/2 & 1 \end{bmatrix}$$
 (1.4)

where n is the number of reference pixels, weight w_i is the inverse of the squared distance to

adjacent pixels, d is a conversion from inches to pixels, px is the projection area in pixels, and

144 Min is a MATLAB (Mathworks) minimization algorithm with free parameters α , β , γ , c, f, and

145 ratio. Each pixel was then associated with a surface coordinate by bilinear interpolation to a

projected mesh of surface points.

Luminance of each pixel lum_i was compensated according to the angle of incidence with the

projection screen to normalize relative intensities:

149

150
$$\theta_i = \tan^{-1} \left(\frac{\|\vec{n}_i \times \vec{v}_i\|}{\vec{n}_i \cdot \vec{v}_i} \right)$$
 (2.1)

151

155

$$w_i = \left|\cos\theta_i\right|^{-1} \tag{2.2}$$

$$lum_i = w_i / \max(w) \tag{2.3}$$

where \vec{n} is the normal vector to the projection surface, \vec{v} is the vector from the projector to the

surface, and w is the compensated luminance weight for each pixel i. Projection area was

restricted such that maximum weights were less than 1.43.

2.1.3 Visual stimulus parameters

- Looming stimuli presented to the fly simulated an object approaching at a constant velocity.
- For a two-dimensional projection, the visual angle subtended by an approaching object can be
- calculated using the following equation:

$$\theta(t) = 2 * \tan^{-1} \frac{r}{tv}$$

157

170

177

178

- where r is the radius of the stimulus, v is the approach velocity, and t is time, where t = 0 at
- 163 collision and t < 0 before collision. These "looming" stimuli were classified by their size to
- speed ratio (r/v, Gabbiani et al., 1999); the angular expansion of a small object approaching
- slowly will be identical to a large object approaching quickly if their r/v are equivalent. For the
- following experiments, we selected an r/v of 40 ms because this elicits the highest escape
- response rate in freely behaving flies (von Reyn et al., 2014). Looming stimuli consisted of a
- black disk expanding from an initial size of 10° to a final size of 78° and the 78° disk was held
- static for 1 second before returning to a white screen (Figure 1B).

2.1.4 Assay control and data acquisition

- 171 Assay control was implemented using custom MATLAB scripts in conjunction with the
- Wavesurfer data acquisition package for MATLAB (http://wavesurfer.janelia.org/) and the
- Psychophysics Toolbox extensions (http://psychtoolbox.org/, Brainard, 1997; Kleiner et al.,
- 2007; Pelli, 1997). Image acquisition was performed by custom C++ script implementing the
- Point Grey acquisition API and buffering to PC memory. Temperature sensor and wing stop
- apparatus were controlled using a PIC microcontroller (Figure 1C).

2.2 Experimental procedures

2.2.1 Fly Stocks

- 179 Drosophila were raised on standard cornmeal/molasses medium at a room temperature of
- approximately 21°C. All experiments were performed on 2-6 day old females between the
- times of 11:00 and 19:00. All genotypes used in this study are listed below:

Label	Genotype	Source
GF-split-	R68A06_p65ADZp (attP40);	(von Reyn et al., 2014)
GAL4	R72E01_ZpGdbd (attP2)	
L1-L2-	R48A08_p65ADZp (attP40);	(Tuthill et al., 2013)
split-GAL4	R29G11_ZpGdbd (attP2)	
UAS-	pJFRC49-10xUAS-IVS-eGFP-	(Pfeiffer et al., 2010; von Reyn et al., 2014; new
Kir2.1	Kir2.1 Su(Hw)attP6/cyo	landing site courtesy of Michael Reiser, Janelia
		Research Campus)
CSMH	Canton S wild type	Martin Heisenberg, University of Wurzburg

Label	Genotype	Figures
Kir X CS	w^+/w^+ ; pJFRC49-10xUAS-IVS-eGFP-Kir2.1 (Su(Hw)attP6)/+; +/+	2-6
CS X L1L2	w/w ⁺ ; R48A08_p65ADZp (attP40)/+; R29G11_ZpGdbd (attP2)/+	2-6
CS X GF	w/w^{+} ; R68A06 p65ADZp (attP40)/+; R72E01 ZpGdbd (attP2)/+	2-6

Kir X L1L2	w/w ⁺ ; pJFRC49-10xUAS-IVS-eGFP-Kir2.1 (Su(Hw)attP6)/R48A08_	
	p65ADZp (attP40); R29G11 ZpGdbd (attP2)	
Kir X GF	w/w^+ ; pJFRC49-10xUAS-IVS-eGFP-Kir2.1 (Su(Hw)attP6)/R68A06	
	p65ADZp (attP40); R72E01 ZpGdbd (attP2)	

Table 1: Experimental fly stocks and crosses.

183 184 185

196

210

2.2.2 Experimental Protocol

Cold anesthetized flies were tethered with UV glue to a 0.1 mm tungsten wire centered at the top of their thorax. After a greater than 30 minute recovery period, flies were centered in front of the escape assay screen via a 3-axis mechanical manipulator. Flies were next acclimated for 30 minutes in front of the fully illuminated screen (white) before looming experiments were initiated. For most experiments, flies were presented 20 trials of a single looming stimulus at an interval of 15 seconds. For Kir X L1L2 flies, an almost complete elimination of escape responses reduced the needed statistical power and limited useful quantification of their escape

responses to the escape rates for first three trials. Therefore, a subset of Kir X L1L2 flies only

received 5 looming stimuli presentations. A wingstop apparatus was engaged 6 seconds after

the start of each trial to ensure cessation of flight before the following trial.

2.2.3 Behavior annotations

In this study, we analyzed the takeoff escape response of non-flying, tethered *Drosophila* to

looming stimuli. In freely behaving flies, takeoff escape consists of a sequence of components

that occur prior to the fly loosing contact with the ground (Card and Dickinson, 2008). Here,

we annotated three components from this sequence: wing elevation, leg extension, and wing

201 depression (Figure 1D).

Behavioral responses were manually scored from video data. The 'wing raise' component was

defined as the first frame of visible movement preceding a flight initiation, 'wing depression' the

first frame of visible downward movement, and the leg extension component the first frame of

downward movement of the mesothoracic legs preceding a rapid, full leg extension (here

referred to as a 'leg kick'). Subsets of trials were annotated by individuals blinded to the

207 experimental genotypes.

208 Trials in which the fly was already flying during the stimulus presentation were excluded from

analysis (6.4% of trials). Flies which experienced technical faults were also excluded.

2.2.4 Data analysis and statistics

211 Statistical analyses were performed in MATLAB with the exception that Fisher's exact test was

performed by Monte Carlo simulation in R. Escape sequence distributions were fit with a

Gaussian mixture model with 3 Gaussians present using the Expectation Maximization

algorithm with initial conditions set for equally weighted Gaussian distributions.

Logistic regressions were performed using MATLABs general linear model package, $\ln \frac{p}{1-p} =$

 $\ln b_0 + trial \ln b_1$, where p is occurrence likelihood, trial is the trial number, and b is the

regression parameter vector. Pseudo R² calculated by Cox and Snell's method (Cox and Snell

218 1989).

219

220

221

3. RESULTS AND DISCUSSION

3.1 Tethered escape assay recapitulates free behavior escape

- To provide a useful alternative or complement to free behavior escape assays, our tethered assay should recapitulate the characteristics of escape in freely behaving flies. Tethered flies should be capable of escaping in response to looming stimuli, display a sequence of actions prior to flight initiation that produce both short and long duration escapes, and rely on the same
- neural circuits that drive escapes in freely behaving flies.

- To compare escapes in our tethered assay to those of freely behaving flies, we first measured 228 the takeoff rates in all control genotypes (Supplemental Figure 1) during the initial three 229 230 looming stimulus trials (Figure 2A). We found that within these early trials, flies escaped at a rate of 73.4% (95% confidence interval 66.3% to 79.4%), within the range reported previously 231 for freely behaving flies (de Vries and Clandinin, 2012; von Reyn et al., 2014, 2017). Next, we 232 investigated the duration of preparatory actions preceding flight initiation. In freely behaving 233 flies, this "escape sequence duration" is bimodally distributed: for a respective r/v, there is 234 some probability that a fly will select a long duration escape, where the fly spends preparation 235 time to fully raise its wings, or a short duration escape, where a takeoff occurs before the wings 236 237 are fully raised (von Reyn et al., 2014). In our tethered assay, we measured this duration from the start of wing motion to the start of wing depression (Figure 1D). Across control flies, the 238 data appear consistent with the bimodal distribution of responses previously observed in freely 239
- behaving flies (Figure 2B). We therefore conclude our assay is effective in eliciting
- probabilistic escape responses.

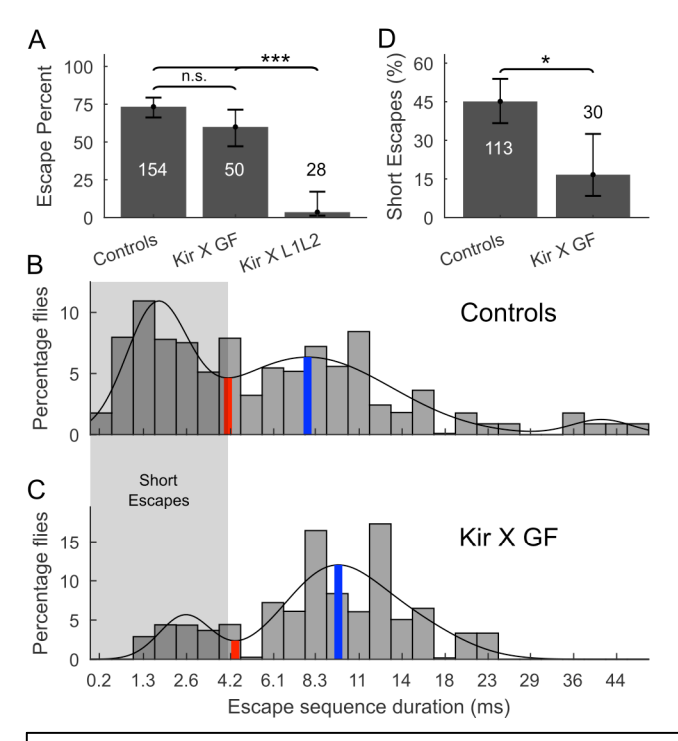


Figure 2: Tethered fly escape response to initial stimulus presentations. (A) Overall escape percentages for the first three stimulus presentations in control, GF silenced (Kir X GF), or L1-L2 silenced (Kir X L1L2) flies (n=trials as indicated, error bars represent 95% CI, χ^2 test of homogeneity). (B) Distribution of the duration of escape sequences, in control flies, across the first three stimulus trials, as measured from the start of wing motion to the start of wing depression. Short escape threshold indicated with red bar, as determined by the intersection of multiple Gaussian fits at 4.0 ms. Peak of 2^{nd} distribution indicated with blue bar (n=113 trials). (C) Distribution of the duration of escape sequences, in GF silenced flies, as described in B (n = 30 trials). For all panels, *=p < .05, **=p < 1x10⁻³. (D) Percentage of short escapes (n=trials as indicated in the panel, error bars represent 95% CI, χ^2 test of homogeneity).

We investigated whether the neural circuit components driving escapes in freely behaving flies also contribute to escapes in tethered flies. In freely behaving flies, all looming evoked escapes require lamina monopolar cells 1 and 2 (L1-L2) that are the inputs to on and off motion vision circuits (Takemura et al., 2013). Approximately 3 synapses downstream of L1 and L2, two large sensorimotor interneurons called the giant fibers (GF) are required for short but not long duration escapes (von Reyn et al., 2014). Using an L1-L2 split-Gal4 driver line (Pfeiffer et al., 2010; Tuthill et al., 2013), we silenced L1 and L2 by selectively expressing inwardly rectifying potassium channels Kir2.1 (Baines et al., 2001; Johns et al., 1999; Pfeiffer et al., 2012). We found that L1 and L2 silencing abolished tethered fly takeoffs to visual stimuli (Figure 2A). Following a similar strategy, we used a GF-split-Gal4 driver to selectively silence the GFs. As expected, GF silencing significantly reduced the percentage of short duration escapes (Figures 2C- 2D) without decreasing overall takeoff rates (Figure 2A). These data are in agreement with

silencing results in freely behaving flies that experience a single visual stimulus presentation: L1-L2 silencing abolishes all free fly takeoffs (von Reyn et al., 2017) and GF silencing abolishes free fly short escapes while alternative, parallel escape circuits maintain overall escape rates (von Reyn et al., 2014). Our data therefore support that the neural circuit mechanisms underlying escape behavior are conserved in our tethered assay.

3.2 Escape percentages decrease with repeated stimulus presentations

One significant advantage our tethered assay provides over free behavior assays is the ability to examine fly behavior across multiple presentations of an expanding visual stimulus. We therefore next investigated how the escape response changes with repeated stimulus trials (20 trials per fly). When comparing the first five trials to the last five trials (Figure 3A), we found a significant decrease in the escape frequency for both control and GF silenced flies. Across trials, this decline in escape frequency was well fit with a logistic regression model (Figure 3B).

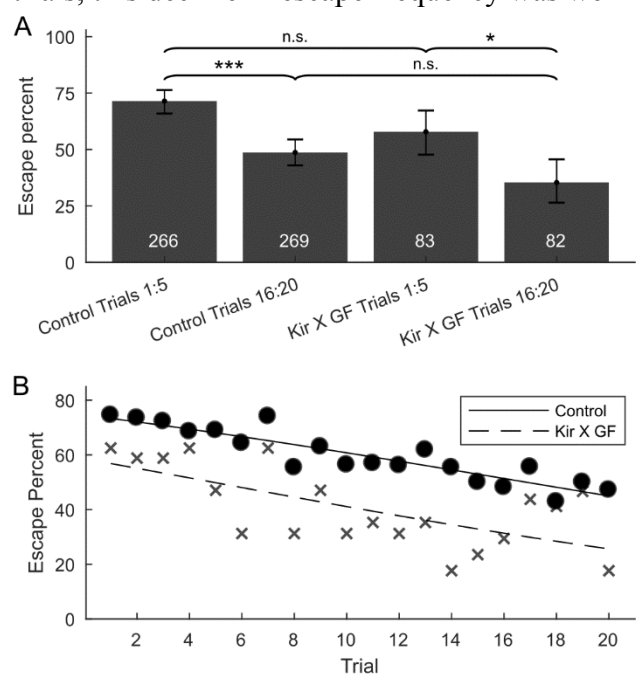


Figure 3: Escape percentages decrease with repeated stimulus trials. (A) Escape response decreased significantly when comparing the first five to last five trials in both controls and GF silenced flies. (n = trials as indicated, χ^2 test of homogeneity). (B) Flies rapidly decreased their responsiveness over the course of trials. (See Supplemental Table 1 for logistic regression parameters). Pseudo R²=0.82, 0.44 for control and Kir X GF, respectively. Escape responses with GF silencing decreased similarly to controls (p = .77 logistic regression). For all panels, *=p < .05, ***= $p < 1 \times 10^{-5}$.

We next investigated how genetically silencing the GF affected escape rates across trials. Similar to control flies, we found a significant decrease in the escape rate when comparing the first five to last five trials (Figure 3A). Despite a lower absolute escape rate, the rate of decline was not significantly different in control and GF silenced flies. This response is similar to

habituation occurring in other visually-evoked *Drosophila* behaviors and is hypothesized to occur within neurons underlying sensory integration (Wittekind and Spatz, 1988). If escape habituation rates are similar across all escape circuits, our data may support that habituation occurs at a location of sensory processing common to all escape circuits.

3.3 Repeated stimulus presentations bias action selection towards long duration escapes After witnessing a significant decrease in escape rates across trials, we next investigated how multiple stimulus presentations alter the distribution of escape sequence durations. In control flies, we found the distribution of the escape sequence durations for the first 5 trials to be significantly different from the last 5 trials (Wilcoxon rank-sum test, Figure 4A and 4B). The percentage of trials eliciting a short duration escape decreased with trial number, while the percentage of trials classified as long did not decrease significantly (Figure 4C-D). This resulted in an overall increase in probability of a long duration escape, if the fly decided to escape, and a significant increase in the average duration of escapes for later trials (Figure 4A and 4B and Figure 5 inset). Our data therefore suggest that flies become biased towards long escapes of increasing duration with repeated stimulus presentations.

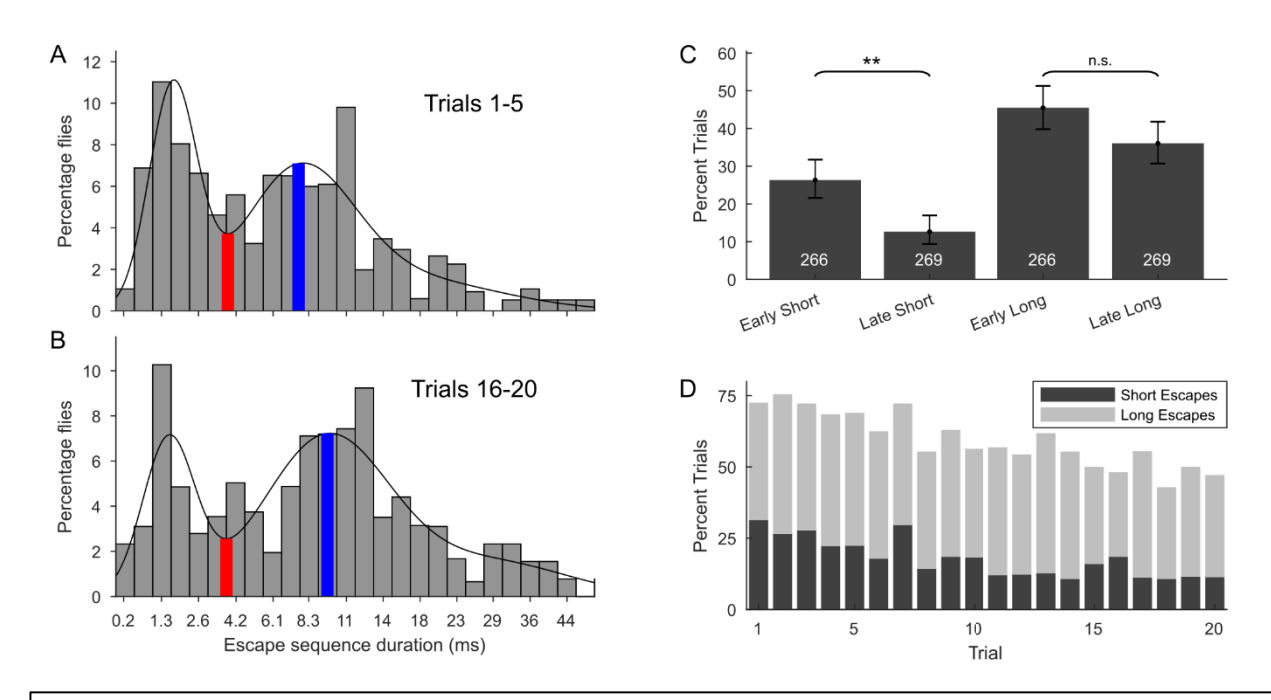


Figure 4: The distribution of escape sequence durations shifts to longer durations with repeated stimulus trials. (A) Escape sequence duration of control fly escapes occurring in trials 1:5. (n = 189 trials). (B) Escape sequence duration for escapes during trials 16:20 (n = 129). (C) The percentage of trials resulting in short or long duration responses in early (1:5) and late (16:20) stimulus presentation trials. (χ^2 test of homogeneity, **= p < 1x10⁻³). (D) Proportion of short but not long duration escapes decreased steadily over trials (logistic regression, odds ratio 0.96 ± 0.016 , n = 60 flies, 24-40 escapes per trial, median 32.5).

This shift towards long duration escapes with repeated stimulus presentation could emerge from at least two possible mechanisms that need not be mutually exclusive. First, the parallel pathways that drive escape behavior could fatigue/habituate at different rates. Similar results have been observed in the tailflip escape of the cravfish, where non-giant mediated escapes decrease more rapidly than Lateral Giant mediated escapes (Reichert and Wine, 1983). Alternatively, an increase in long escapes could emerge from alterations in the latency of activation between parallel circuits driving escapes. Modeling studies suggest both GF and alternate escape circuits are activated when a predator approaches (von Reyn et al., 2014). Whether a long or short duration escape occurs depends on the relative spike timing of each pathway. If an alternative pathway initiates wing raising and then completes an escape takeoff prior to a GF spike, the escape is long. If the GF spikes before alternate pathways are able to initiate a behavior, leg extension and wing depression occur in the absence of wing raising and the escape is short. However, if the GF spikes while an alternative pathway has already engaged wing raising, a GF-mediated, long duration escape occurs. An increase in long duration escapes may therefore indicate an increase in stimulus response latency for alternate escape circuits. Delayed spiking in alternate circuits, as long as GF spike time remains consistent, would produce more GF-mediated, long duration escapes.

3.4 Response latency increases with repeated stimulus presentations

We therefore next investigated how the latency of initiation of wing raising and initiation of wing depression, with respect to the start of each stimulus presentation, changes across trials. We found a significant increase in response latency for both escape components, that could be fit with an asymptotic model (Figure 5). Although an additional delay of 64ms on average between the initial and final trials may seem small, components of the escape behavior occur on the scale of milliseconds (von Reyn 2014). A spike in the GF, for example, activates the muscles for wing depression within 2ms (Allen and Godenschwege, 2010). Additionally, this asymptotic increase in response initiation is similar to that of visually evoked landing response habituation (Wittekind and Spatz, 1988). These data therefore suggest that repeated stimulus presentations alter parallel circuit activation latencies within a relevant timescale to affect the probability of a short or long duration escape. These data also warrant future electrophysiological studies to determine the biological source of delayed response latency and test our hypothesis posited above.

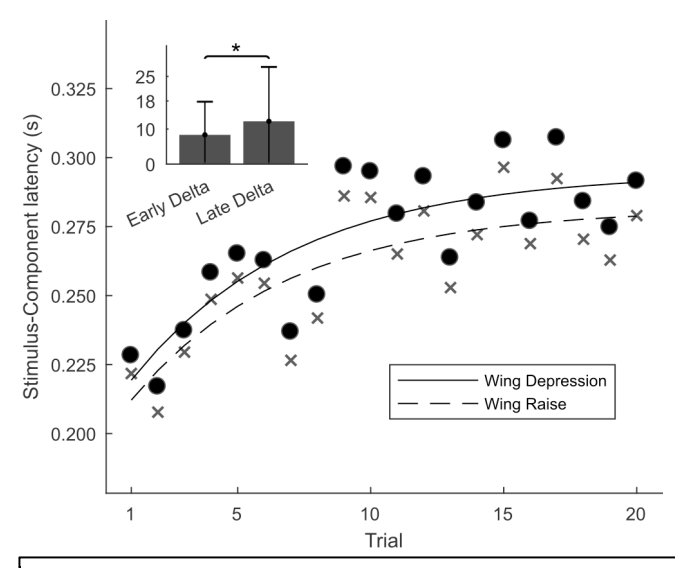
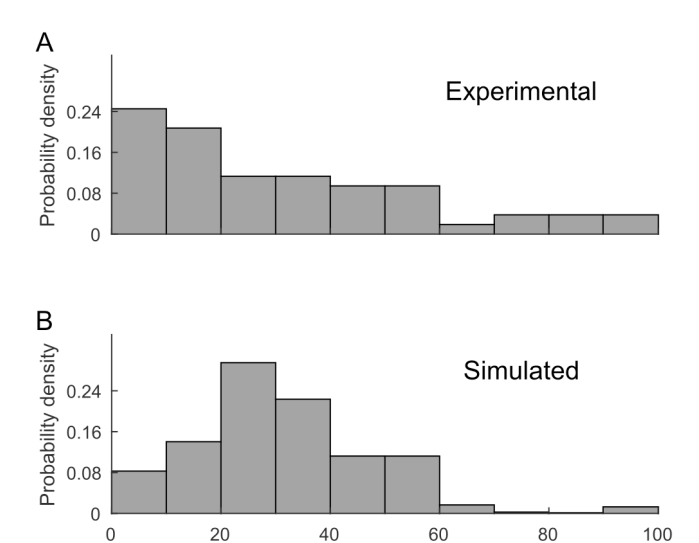


Figure 5: Mean escape sequence wing raising and wing depression latencies with respect to stimulus onset time. Onset latency increases asymptotically over the course of trial presentations: $0.2 + 0.08(1 - e^{-.17*trial})$. Inset: Mean duration of interval (ms) between wing raise and depression increases significantly from early (1:5) to late (16:20) trials (*= p < .05, t test, error bars indicate 95% confidence interval).

3.5 Individual fly action selection bias

Our tethered escape assay also provides the advantage to investigate individual biases in escape responses. We first examined how the probability of initiating an escape differs across individual flies. Our data indicate a small inverse correlation between the percentage of a fly's escapes which utilize the short mode response and the percentage of trials in which it responds (Supplemental Figure 2).



Percent short escapes

<u>Figure 6: Individual biases in action selection.</u> **(A)** Distribution of fly short escape percentages for controls. Escape response type selection was significantly heterogeneous among flies ($p << 1x10^{-7}$, Fisher's exact test, n=53 flies). **(B)** Expected distribution under assumption of stochastic escape type selection with population mean.

Finally, we utilized our assay to investigate individuality in action selection. In selecting a short or long duration escape, individual flies could be hard wired for a given escape response, yielding a fly invariant escape selection. Alternatively, a homogeneous populations of flies may stochastically select escape responses with similar distributions, as seen with left vs right handedness in locomotor behaviors (Ayroles et al., 2015). To test these two hypotheses, we plotted the distribution of the percentage of short duration escapes for individual flies and compared this to a simulated distribution of a homogeneous population (Figure 6). We found that the percentage of short escapes is highly non-homogeneous (p << 1e-7), indicating that individual flies exhibit significant bias toward a given escape type, rather than the population average distribution. As the mechanisms that underlie behavioral individuality remain poorly understood, our assay presents a novel way to explore individuality in action selection at the high level of detail afforded by a genetically tractable animal.

4. CONCLUSION

In conclusion, our tethered escape assay offers a simple method for flexibly evaluating looming-evoked escape responses in flies, effectively recapitulating critical features of the free behavior escape response. The ability to repeatedly record the response of individual flies provides a number of benefits, including the ability to analyze both individual and population behavioral variability and to measure changes in the response over time. The assay also enables the investigator to capture the fly after behavior experiments for further analysis of circuit structure or genetic construct expression, or to perform additional testing, such as calcium imaging or electrophysiology.

In addition to validating our behavior assay, our results shed further light on the interaction between parallel circuits driving action selection in *Drosophila* escape behavior. First, we find

the escape frequency declines with repeated stimulus trials, and that this decrease is similar even in the absence of the GF. The question of whether the reduction in escapes is due to synaptic habituation or motor fatigue is an area for future investigation. Next, we find a decrease in overall escapes is attributed primarily to a decrease in short duration escape responses. Since non-GF mediated escapes decrease with repeated stimulus presentation, these results suggest GF long escapes must increase to enable a stable percentage of long duration escapes in control flies that warrants further investigations. Finally, our results indicate that the binomial distribution in escape sequence duration manifests through a bias in action selection within individual flies, rather than a randomized selection of short or long escapes from a set probability distribution. Whether genetic or circuit mechanisms contribute to this bias remains to be determined.

Future work with this assay may include identification of multisensory integration components, such as the role of antennal stimulation or tarsal contact in modulating escape responses. Although the absence of a physical substrate for the fly to interact with during escapes does not interfere with the presence of both short or long wing preparations in our assay, proprioceptive feedback likely contributes to leg posture and extension during free behavior escapes (Card and Dickinson, 2008) and may also differentially interact with descending and motor circuits mediating the behavior. Our assay fortunately permits the addition of various substrates for tarsal contact to dissect these interactions in future investigations. Additionally, the circuit mechanisms underlying individual response variation may provide an avenue for future investigation, both regarding their stability and persistence over time and the cellular mechanisms responsible for them. Research in this area may help to illuminate general mechanisms of behavioral modulation and variability more generally.

Funding sources:

This material is based upon work supported by the National Science Foundation under Grant No. CBET-1747506

- 414 5. REFERENCES
- 415 Allen, M.J., and Godenschwege, T.A. (2010). Electrophysiological Recordings from the Giant Fiber
- 416 System. Cold Spring Harb. Protoc. 2010, pdb.prot5453.
- 417 Allen, M.J., Godenschwege, T.A., Tanouye, M.A., and Phelan, P. (2006). Making an escape:
- development and function of the Drosophila giant fibre system. Semin. Cell Dev. Biol. 17, 31–41.
- 419 Ayroles, J.F., Buchanan, S.M., O'Leary, C., Skutt-Kakaria, K., Grenier, J.K., Clark, A.G., Hartl, D.L., and
- 420 Bivort, B.L. de (2015). Behavioral idiosyncrasy reveals genetic control of phenotypic variability. Proc.
- 421 Natl. Acad. Sci. 112, 6706-6711.
- 422 Bahl, A., Ammer, G., Schilling, T., and Borst, A. (2013). Object tracking in motion-blind flies. Nat.
- 423 Neurosci. *16*, 730–738.
- 424 Baines, R.A., Uhler, J.P., Thompson, A., Sweeney, S.T., and Bate, M. (2001). Altered electrical properties
- in Drosophila neurons developing without synaptic transmission. J. Neurosci. Off. J. Soc. Neurosci. 21,
- 426 1523-1531.
- 427 Brainard, D.H. (1997). The Psychophysics Toolbox. Spat. Vis. 10, 433–436.
- 428 Brand, A.H., and Perrimon, N. (1993). Targeted gene expression as a means of altering cell fates and
- 429 generating dominant phenotypes. Dev. Camb. Engl. 118, 401–415.
- 430 Card, G., and Dickinson, M.H. (2008). Visually mediated motor planning in the escape response of
- 431 Drosophila. Curr. Biol. CB 18, 1300–1307.
- 432 Clark, D.A., Bursztyn, L., Horowitz, M., Schnitzer, M.J., and Clandinin, T.R. (2011). Defining the
- 433 computational structure of the motion detector in Drosophila. Neuron 70, 1165–1177.
- De Franceschi, G., Vivattanasarn, T., Saleem, A.B., and Solomon, S.G. (2016). Vision Guides Selection of
- 435 Freeze or Flight Defense Strategies in Mice. Curr. Biol. 26, 2150–2154.
- de Vries, S.E.J., and Clandinin, T.R. (2012). Loom-Sensitive Neurons Link Computation to Action in the
- 437 Drosophila Visual System. Curr. Biol. 22, 353–362.
- Dunn, T.W., Gebhardt, C., Naumann, E.A., Riegler, C., Ahrens, M.B., Engert, F., and Del Bene, F. (2016).
- 439 Neural Circuits Underlying Visually Evoked Escapes in Larval Zebrafish. Neuron 89, 613–628.
- 440 Eaton, R.C., Bombardieri, R.A., and Meyer, D.L. (1977). The Mauthner-initiated startle response in
- 441 teleost fish. J. Exp. Biol. *66*, 65–81.
- 442 Eaton, R.C., DiDomenico, R., and Nissanov, J. (1991). Role of the Mauthner cell in sensorimotor
- integration by the brain stem escape network. Brain. Behav. Evol. 37, 272–285.
- Edwards, D.H., Heitler, W.J., and Krasne, F.B. (1999). Fifty years of a command neuron: the
- neurobiology of escape behavior in the crayfish. Trends Neurosci. 22, 153–161.
- 446 Fotowat, H., Fayyazuddin, A., Bellen, H.J., and Gabbiani, F. (2009). A novel neuronal pathway for
- visually guided escape in Drosophila melanogaster. J. Neurophysiol. 102, 875–885.

- 448 Gabbiani, F., Krapp, H.G., and Laurent, G. (1999). Computation of Object Approach by a Wide-Field,
- 449 Motion-Sensitive Neuron. J. Neurosci. 19, 1122–1141.
- 450 Hemmi, J.M., and Pfeil, A. (2010). A multi-stage anti-predator response increases information on
- 451 predation risk. J. Exp. Biol. 213, 1484–1489.
- 452 Hemmi, J.M., and Tomsic, D. (2015). Differences in the escape response of a grapsid crab in the field
- 453 and in the laboratory. J. Exp. Biol. *218*, 3499–3507.
- 454 Herberholz, J. (2009). Recordings of Neural Circuit Activation in Freely Behaving Animals. J. Vis. Exp.
- 455 JoVE.
- 456 Holmqvist, M.H., and Srinivasan, M.V. (1991). A visually evoked escape response of the housefly. J.
- 457 Comp. Physiol. A 169, 451–459.
- Johns, D.C., Marx, R., Mains, R.E., O'Rourke, B., and Marbán, E. (1999). Inducible genetic suppression of
- 459 neuronal excitability. J. Neurosci. Off. J. Soc. Neurosci. 19, 1691–1697.
- 460 Klapoetke, N.C., Nern, A., Peek, M.Y., Rogers, E.M., Breads, P., Rubin, G.M., Reiser, M.B., and Card,
- 461 G.M. (2017). Ultra-selective looming detection from radial motion opponency. Nature 551, 237–241.
- 462 Kleiner, M., Brainard, D., Pelli, D., Ingling, A., Murray, R., and Broussard, C. (2007). What's new in
- 463 psychtoolbox-3. Perception 36, 1–16.
- Lai, S.-L., and Lee, T. (2006). Genetic mosaic with dual binary transcriptional systems in Drosophila. Nat.
- 465 Neurosci. *9*, 703–709.
- Liu, K.S., and Fetcho, J.R. (1999). Laser ablations reveal functional relationships of segmental hindbrain
- neurons in zebrafish. Neuron *23*, 325–335.
- 468 Maimon, G., Straw, A.D., and Dickinson, M.H. (2010). Active flight increases the gain of visual motion
- processing in Drosophila. Nat. Neurosci. 13, 393–399.
- 470 Niven, J.E., Vahasoyrinki, M., Kauranen, M., Hardie, R.C., and al, et (2003). The contribution of Shaker
- 471 K+ channels to the information capacity of Drosophila photoreceptors. Nat. Lond. 421, 630–634.
- 472 Oliva, A., and Torralba, A. (2007). The role of context in object recognition. Trends Cogn. Sci. 11, 520–
- 473 527.
- 474 Pelli, D.G. (1997). The VideoToolbox software for visual psychophysics: transforming numbers into
- 475 movies. Spat. Vis. 10, 437–442.
- 476 Pfeiffer, B.D., Jenett, A., Hammonds, A.S., Ngo, T.-T.B., Misra, S., Murphy, C., Scully, A., Carlson, J.W.,
- Wan, K.H., Laverty, T.R., et al. (2008). Tools for neuroanatomy and neurogenetics in Drosophila. Proc.
- 478 Natl. Acad. Sci. 105, 9715–9720.
- 479 Pfeiffer, B.D., Ngo, T.-T.B., Hibbard, K.L., Murphy, C., Jenett, A., Truman, J.W., and Rubin, G.M. (2010).
- 480 Refinement of tools for targeted gene expression in Drosophila. Genetics 186, 735–755.

- 481 Pfeiffer, B.D., Truman, J.W., and Rubin, G.M. (2012). Using translational enhancers to increase
- transgene expression in Drosophila. Proc. Natl. Acad. Sci. 109, 6626–6631.
- 483 Reichert, H., and Wine, J.J. (1983). Coordination of lateral giant and non-giant systems in crayfish
- 484 escape behavior. J. Comp. Physiol. 153, 3–15.
- 485 Reiser, M.B., and Dickinson, M.H. (2008). A modular display system for insect behavioral neuroscience.
- 486 J. Neurosci. Methods *167*, 127–139.
- 487 von Reyn, C.R., Breads, P., Peek, M.Y., Zheng, G.Z., Williamson, W.R., Yee, A.L., Leonardo, A., and Card,
- 488 G.M. (2014). A spike-timing mechanism for action selection. Nat. Neurosci. 17, 962–970.
- 489 von Reyn, C.R., Nern, A., Williamson, W.R., Breads, P., Wu, M., Namiki, S., and Card, G.M. (2017).
- 490 Feature Integration Drives Probabilistic Behavior in the Drosophila Escape Response. Neuron 94, 1190-
- 491 1204.e6.
- 492 Takalo, J., Piironen, A., Honkanen, A., Lempeä, M., Aikio, M., Tuukkanen, T., and Vähäsöyrinki, M.
- 493 (2012). A fast and flexible panoramic virtual reality system for behavioural and electrophysiological
- 494 experiments. Sci. Rep. 2.
- Takemura, S., Bharioke, A., Lu, Z., Nern, A., Vitaladevuni, S., Rivlin, P.K., Katz, W.T., Olbris, D.J., Plaza,
- 496 S.M., Winston, P., et al. (2013). A visual motion detection circuit suggested by Drosophila
- 497 connectomics. Nature 500, 175–181.
- 498 Trimarchi, J.R., and Schneiderman, A.M. (1995). Initiation of flight in the unrestrained fly, Drosophila
- 499 melanogaster. J. Zool. 235, 211–222.
- 500 Tuthill, J.C., Nern, A., Holtz, S.L., Rubin, G.M., and Reiser, M.B. (2013). Contributions of the 12 neuron
- 501 classes in the fly lamina to motion vision. Neuron 79, 128–140.
- Wittekind, W.C., and Spatz, H.C. (1988). Habituation of the Landing Response of Drosophila. In
- 503 Modulation of Synaptic Transmission and Plasticity in Nervous Systems, (Springer, Berlin, Heidelberg),
- 504 pp. 351–368.
- Yamaguchi, S., Desplan, C., and Heisenberg, M. (2010). Contribution of photoreceptor subtypes to
- 506 spectral wavelength preference in Drosophila. Proc. Natl. Acad. Sci. 107, 5634–5639.
- 507 Yilmaz, K. (2013). Comparison of Quantitative and Qualitative Research Traditions: epistemological,
- theoretical, and methodological differences. Eur. J. Educ. 48, 311–325.
- 509
- 510
- 511
- 512
- 513